Environment International 153 (2021) 106527

Contents lists available at ScienceDirect

Environment International

journal homepage: www.elsevier.com/locate/envint

Use of biochar to reduce mercury accumulation in *Oryza sativa* L: A trial for sustainable management of historically polluted farmlands

Yi Man [a,b], Bo Wang [a,b], Jianxu Wang [a,c,*], Michal Slaný [d,e], Haiyu Yan [a,*], Ping Li [a], Ali El-Naggar [f], Sabry M. Shaheen [g,h,i], Jörg Rinklebe [g,j], Xinbin Feng [a,c]

[a] State Key Laboratory of Environmental Geochemistry, Institute of Geochemistry, Chinese Academy of Sciences, Guiyang 550081, PR China
[b] University of Chinese Academy of Sciences, Beijing 100049, PR China
[c] CAS Center for Excellence in Quaternary Science and Global Change, Xi'an, 710061, China
[d] Institute of Inorganic Chemistry, Slovak Academy of Sciences, Dúbravská cesta 9, 84536 Bratislava, Slovakia
[e] Institute of Construction and Architecture, Slovak Academy of Sciences, Dúbravská cesta 9, 84503 Bratislava, Slovakia
[f] Department of Soil Sciences, Faculty of Agriculture, Ain Shams University, Cairo 11241, Egypt
[g] University of Wuppertal, School of Architecture and Civil Engineering, Institute of Foundation Engineering, Water- and Waste-Management, Laboratory of Soil- and Groundwater-Management, Pauluskirchstraße 7, 42285 Wuppertal, Germany
[h] Department of Arid Land Agriculture, Faculty of Meteorology, Environment, and Arid Land Agriculture, King Abdulaziz University, Jeddah 21589, Saudi Arabia
[i] Department of Soil and Water Sciences, Faculty of Agriculture, University of Kafrelsheikh, 33516 Kafr El-Sheikh, Egypt
[j] University of Sejong, Department of Environment, Energy and Geoinformatics, Guangjin-Gu, Seoul 05006, Republic of Korea

ARTICLE INFO

Handling Editor: Hefa Cheng

Keywords:
Green remediation
Mercury contaminated paddy soils
Renewable materials
Human health
Safe rice production

ABSTRACT

Mitigating the risk of mercury (Hg) contamination in rice soils using environmental friendly amendments is essential to reducing the probable daily intake (PDI) of MeHg via rice consumption. Here, we examined the impacts of different doses (0% (control), 0.6% and 3%) of rice hull-derived biochar (RHB) and mixture of wheat-rice straw-derived biochar (RWB) on the fractionation, phytoavailability, and uptake of total (THg) and methyl Hg (MeHg) by rice in Hg-polluted soil (THg = 78.3 mg kg^{-1}) collected from Wanshan Hg mining area. Both biochars increased rice biomass up to 119% as compared to control. Application of RHB and RWB significantly ($P \leq 0.05$) decreased bioavailable Hg (soluble and exchangeable and specifically-sorbed fractions) concentrations by 55–71% and 67–72%, respectively. The addition of RHB significantly decreased MeHg concentrations in the soil. However, RWB (particularly at 3%) increased significantly MeHg concentrations in the soil as compared to the control and RHB treatments, likely due to the increased abundance of Hg-methylation microorganisms (e.g., *Geobacter* spp., *Nitrospira* spp.) in the RWB treatments. Both RHB and RWB significantly decreased MeHg concentrations in the rice grain by 55–85%. We estimated a reduction of the PDI of MeHg from 0.26 μg kg^{-1} bw $d^{-1}$of control to below the reference dose (0.1 μg kg^{-1} bw d^{-1}) of two biochar treatments. Our results highlight the potentiality of RWB and RHB for mitigating MeHg accumulation in rice and reducing PDI of MeHg via rice consumption, which offers a sustainable approach for management of Hg-polluted soils.

1. Introduction

Mercury (Hg) is a toxic and ubiquitous element revealing a high mobility and bioaccumulation in the environment (Driscoll et al., 2013). Methylmercury (MeHg) is a neurotoxin (Sommer et al., 2016), as revealed by horrible historical MeHg pollution events such as Minamata disease in Japan in 1956, and MeHg poisoning via MeHg-polluted wheat grains in Iraq in 1971 (NRC 2000). Both natural and anthropogenic sources contribute to Hg contamination of the environment (Wang et al., 2012). Anthropogenic Hg contamination sources include fossil fuel combustion, non-ferrous metals smelting, caustic soda production and production of cement, Hg ores retorting, etc. (Wu et al., 2016).

Minamata convention on Hg entered into force since 2017, and it aims to reduce anthropogenic Hg emissions and human exposure to Hg (Wang et al., 2020a). In China, non-ferrous metals mining activities, polyvinyl chloride production, and industrial activities (Zhang et al.,

* Corresponding authors.
E-mail addresses: wangjianxu@vip.gyig.ac.cn (J. Wang), michal.slany@savba.sk (M. Slaný), yanhaiyu@vip.gyig.ac.cn (H. Yan), shaheen@uni-wuppertal.de (S.M. Shaheen), rinklebe@uni-wuppertal.de (J. Rinklebe).

https://doi.org/10.1016/j.envint.2021.106527
Received 28 October 2020; Received in revised form 5 March 2021; Accepted 12 March 2021
Available online 27 March 2021

2015) lead to a widespread contamination of soil toxic elements including Hg. A recent national-wide investigation on Hg concentration in soil samples cross entire China indicated that about 1.6% of the studied sites exceed the maximum allowable Hg content in soils defined by Chinese government (Ministry of Environmental Protection and Ministry of Land and Resources, 2014). An obvious risk associated with cultivation in polluted farmland is the accumulation of Hg in edible sections of crops (Liu et al., 2019a; Millán et al., 2013; Xing et al., 2019). The risk is higher in paddy fields where inorganic Hg can be converted to MeHg by microorganism (e.g., sulfate reducing bacteria, etc.) (Vishnivetskaya et al., 2018). In fact, the contamination of rice grain with MeHg at Hg polluted sites has been documented worldwide (Liu et al., 2019b). Since more than half of the world's population relies on rice as a major staple food (Muthayya et al., 2014), there is an increasingly global concern on MeHg dietary exposure via rice consumption (Jiménez-Moreno et al., 2018; Rothenberg et al., 2014). The probable daily intake (PDI) of MeHg via rice consumption for inhabitants at Hg mining regions exceeds the reference dose (0.1 μg kg^{-1} bw d^{-1}) defined by U.S Environmental Protection Agency (EPA) (Feng et al., 2008; USEPA 1997; Zhang et al., 2010). There was great human health risks associated with rice consumption at contaminated areas/sites (e.g., Hg mining regions, coal-fired power plants zinc and lead smelting sites, chlor-alkali industries, etc.) (Li et al., 2009; Qasim and Motelica-Heino 2014). The urgent intervention and remediation are essential to reducing Hg accumulation in rice grain, and thereby reducing human exposure to MeHg.

Several approaches have been employed for Hg remediation including stabilization/solidification, chemical washing, and electroremediation. However, most of these techniques exhibited drawbacks in maintaining the sustainable management of Hg polluted soils since they are destructive, costive, and time-consuming (Wang et al. 2014). Immobilization methods have received particular attention because they achieve sustainable land use via adding environmental friendly amendments to reduce the bioavailability of pollutants and allow the safe use of agricultural soils (Shaheen et al., 2019). However, the lack of sustainable amendment limits the scale up and application of immobilization methods.

Biochar is produced by pyrolysis of biomass in limited O_2 environment, and it displays great advantages in remediation of polluted soils and mitigation climatic change (El-Naggar et al., 2020). Biochar can absorb heavy metals because of its large surface area, high cation exchange capacity, as well as enrichment of porous structure and surface functional groups (Beesley et al., 2015; Cao et al., 2009; Park et al., 2011). It attracts global interests in heavy metal pollution control due to its cost-effective and environmentally friendly (Namgay et al., 2010). Several pilot studies have been conducted to removing Hg from solutions and gas-phase (Gamboa-Herrera et al., 2020; He et al., 2019; Kong et al., 2011; Lahori et al., 2017; Lee et al., 2006). Biochar can absorb Hg^{2+} through its —OH, —COOH, —NH_2 groups (Dong et al., 2013). Graphite-like domains in the aromatic structure of biochar pyrolyzed at high temperature (e.g., 600 °C) play a dominant role in Hg^{2+} adsorption (Li et al., 2017).

Although much progress had been achieved for inorganic Hg, effect of biochar on $MeHg^{+}$ remains to be addressed (Beckers et al., 2019). MeHg production is a microbially mediated process (Beckers and Rinklebe 2017; Schaefer et al., 2014). Biochar may alter composition and relative abundance of Hg-methylation microorganism because it provides carbon and nutrients. Further, pore structure of biochar may serve as habitat for microorganisms to enhance their reproductions (Palansooriya et al., 2019). The reduction of inorganic Hg bioavailability can inhibit methylation since a small amount of Hg will be available for methylation. The hgcA gene in microorganism was essential for Hg methylation (Parks et al., 2013), and it can be used as a biomarker to reveal the relative abundance and diversity of Hg-methylation microorganisms in soils (Podar et al., 2015; Smith et al., 2015).

We hypothesized that biochar addition to soil will decrease bioavailable Hg in soils, and biochar can also change Hg-methylation bacteria, affecting MeHg production in paddy soils and its uptake by rice plants.

To test this hypothesis, we added rice hull-derived biochar (RHB) and mixture of rice and wheat straw-derived biochar (RWB) at different doses (0% (control), 0.6% and 3% w/w) to a historically Hg polluted paddy soil (THg = 78.3 mg kg^{-1}) collected from Wanshan Hg mining area in China. The overall aim was to explore the potential of RHB and RWB in the sustainable remediation of Hg-polluted farmlands. Particularly, we aimed (1) to examine the impact of different doses of RHB and RWB on the geochemical fractionation and mobilization of Hg in the contaminated paddy soil, (2) to quantify the effect of RHB and RWB amendments on THg and MeHg accumulation and their distributions in the tissues of *Oryza sativa* L., (3) to elucidate the alterations of the microbial community composition by RHB and RWB amendments using 16S rDNA sequencing method, and (4) to assess the impact of remediation on PDI of MeHg and THg via rice consumption for inhabitants at Hg mining areas.

2. Materials and methods

2.1. Biochar production and soil collection

Two biochar samples were produced at 600 °C via a slow pyrolysis of rice hull (RHB) and the mixture of rice straw and wheat straw (RWB), respectively. They were purchased from Jiangsu Huafeng Bioengineering Technology Company. More details of biochar production are described in the supplementary information (SI, section S1). Mercury polluted soil was collected from a polluted paddy field at Dashuixi village close to Wanshan Hg mine in China. About 500 kg of top soils (0 to 20 cm) were collected from a paddy field covering an area of 30 m^2. The soil was air-dried, ground and sieved to < 10 mm prior to experiment and characterization.

2.2. Biochar characterization

The biochar pH was determined with a pH meter (DDS-307, Leici Co., Shanghai, China) in suspension with biochar to deionized water mass ratio of 1: 2.5. Total carbon (TC), total nitrogen (TN), total sulfur (TS) and hydrogen (H) contents were determined using an Organic elemental Analyzer (Vario, Analytik Jena, Germany). Sulfate (SO_4^{2-}) and phosphate (PO_4^{3-}) were determined in suspensions at solid to water ratio of 1:5 using ion chromatograph (ICS-90, Dionex, USA). Total potassium content was measured using an inductively coupled plasma optical emission spectrometer (ICP-OES, Wasst-mpx, Agilent, USA). Organic matter content was determined by potassium dichromate oxidation titration (Wang et al., 2014). The infrared spectra of biochar was obtained by Fourier Transform Infrared (FTIR) spectrometer (Shimadzu IR Affinity-1, Japan) equipped with an IR source, DTGS detector and KBr beam splitter for the mid-IR (MIR) region (4000–400 cm^{-1}). Briefly, about 1 mg of biochar was mixed with 200 mg KBr at a mass ratio of 1:200 in an agate mortar and pressed into a pallet. The scanning electron microscopic images of biochars were taken by a field emission scanning electron microscope with the operational voltage of 20 kV (FEI Quanta 200 FEG, FeiScios Dual Beam, USA). Biochar particles were placed on the black conductive double-sided adhesive tape and mounted on the sample holder. The loosely attached samples were carefully blown away by rubber suction bulb to avoid the falling of samples into electron microscope. The energy dispersive X-ray spectrometer (EDS, USA) spectra of the biochar were obtained with energy dispersive spectroscopy.

2.3. Pot experiment

A series of pot experiment was conducted at the Institute of Geochemistry, Chinese Academy of Sciences, in Guiyang city, Guizhou

province. In total, 15 new plastic pots (25 cm in diameter and 28 cm in height) were randomly divided into five groups, each group contain three pots serving as independent replications. We designated five treatments, including control (untreated soil), 0.6% RHB, 3% RHB, 0.6% RWB, and 3% RWB (Xing et al., 2019). The details for treatments are displayed in the SI (section S2). All pots were kept waterlogged (overlying water is about 3 cm in depth above surface soil) for 30 days for equilibrium and also in order to get closer to the cultivate characteristics of paddy field. Thereafter, three rice seedlings (30-day old, Yixiang 2866) were transplanted into each pot. All rice plants were maintained for 126 days until harvest. During the rice growing season, about 5 g multiple nutrients fertilizer (the contents of N, P and K are more than 45% of total weight) was added to each pot at transplanting stage, tillering stage and panicle stage, respectively. During the experiment, the temperatures ranged between 23 and 28 °C, the relative humidity was 60%-80%, and the concentration of total gaseous Hg in the ambient air was less than 10 ng m^{-3}.

2.4. Plant and soil sample pretreatment and determination

Bulk soil was sampled prior to pot experiment. During rice plant sampling, we cut the plastic pot using knife, and got the entire potted soil and rice plant. We carefully shake off the soil that loosely attached to the roots for 10 min, and collected rhizosphere soil that sticky attached to the roots. After rhizosphere soil sampling, we put the entire roots into tap water and carefully remove the attached the soil particles. Thereafter, the roots were cleaned with tap water and subsequently with deionized water. The aboveground tissue was divided into stalk, leaf and panicle using stainless steel scissors. The rice panicle was further separated into hull, bran, and grain. All tissues were stored in pre-cleaned nylon bags. In the laboratory, rice tissues were washed with running tap water firstly and then thoroughly by deionized water. Roots were further cleaned with 0.01 M EDTA and deionized water (Wang et al., 2020a; Xing et al., 2020). All plants and soil subsamples were frozen at −20 °C, and thereafter freeze-dried using a freeze drier (EYELA, Tokyo, Japan) at −78 °C and 10 Pa for 72 h. Dry biomass of different tissues was recorded by a balance (precision = 0.01 g) prior to grinding to powders by an electric mill (AQ-180E-X, Cixinaiou Electric Appliance Co., China).

Furthermore, rhizosphere soil samples divided into two subsamples, in which one subsample was stored in ziplock bags for chemicals determination, and the other one was put into a sterilized tube and stored in liquid nitrogen to determine the microbial compositions. The freezer-dried soil was ground with a mortal and sieved to pass through a 200 mesh nylon sieve. Before analysis, all prepared samples were individually packed into ziplock bags. The bulk and rhizosphere soil samples were characterized according to the standard methods (Sparks et al., 1996). The analytical methods for soil pH, organic matter, total carbon, hydrogen, oxygen and nitrogen and, as well as sulfate, phosphate, potassium were the same with the methods for biochar. For THg analysis, about 0.1 g soil samples were digested with fresh *aqua regia* (HNO_3: HCl = 1:3, v/v) in water bath at 95 °C for 3 h, while rice tissues (roots, stalks, leaves and grains) were digested with 5 ml concentrated HNO_3 in a water bath at 95 °C for 3 h (Horvat et al., 1991; USEPA 2002). Total Hg concentration in the digested solutions were measured by BrCl oxidation, $SnCl_2$ reduction and cold-vapor atomic fluorescence spectrometer (CVAFS, Brooks Rand Model III, Seattle, USA) according to the USEPA Method 1631 (USEPA 2002). For MeHg determination, about 0.2 g rice tissues were digested with 5 ml 25% KOH solvent at 75 °C for 3 h. During digestion, all tubes were shaken by hands for 10 s every 30 min. As for soil samples, about 0.2 g soil powder was digested with saturated 2 M $CuSO_4$-methanol extraction agents (Liang et al., 1996; USEPA 2001). Thereafter, MeHg in the solution was extracted with CH_2Cl_2(chromatographic purity), back extraction with ultrapure water, conversion of MeHg to methylethyl Hg by ethylation reagent ($NaBEt_4$) and determined by Gas chromatography Cold Vapor Atomic Fluorescence Spectrometry (GC-CVAFS, Brooks Rand model III, Seattle, USA) according to USEPA Method 1630 (USEPA 2001).

The sequential extraction procedure (SEP) was used to determine different geochemical fractions of Hg in soil (Frohne and Rinklebe 2013; Huang et al., 2019). The SEP (Bao et al., 2011; Tessier et al., 1979) operationally differentiated soil Hg into five fractions, including soluble and exchangeable fraction (F1), specifically-sorbed fraction (F2), oxide bound fraction (F3), organic bound (sulfides) fraction (F4) and residual fraction (F5). After each extraction step, the supernatants were separated from the soil by centrifugation at 3500 rpm for 15 min, and then put into clean tubes for analysis (Liu et al., 2019c). The supernatant of F1, F2 and F3 fractions were measured by cold-vapor atomic fluorescence spectrometer, whereas F4 and F5 fractions were measured by cold vapor atomic absorption spectrometry (CVAAS) (F732-VJ, Huaguang instruments, Shanghai, China). More details about SEP are provided in Table S1.

We calculated the probable daily intake (PDI) of total Hg and MeHg via rice consumption for inhabitant at Hg mining regions, and compared the PDI both for control and biochar treatments. More details are displayed in the SI-S3.

Both bioaccumulation factor (BAF) and the translocation factor (TF) are used to indicate the accumulation and translocation of THg and MeHg from soil to rice plants. The BAF refers to the ratio of Hg concentration in plants to the Hg concentration in soils. The TF is calculated as shoot-to-root Hg concentration ratio and is adopted to assess the capacity of plants to translocate Hg from roots to aboveground tissues (Buscaroli 2017; Liu et al., 2020; Pandey et al., 2016). The detailed calculation methods are as follows.

$$BAF = \frac{Hg\ concentration\ in\ rice\ tissues\ (ng\ g^{-1}\ DW)}{Hg\ concentration\ in\ soil\ (ng\ g^{-1}\ DW)}$$

$$TF = \frac{Hg\ concentration\ in\ stalk/leaf/grain (ng\ g^{-1}\ DW)}{Hg\ concentration\ in\ root/stalk/leaf (ng\ g^{-1}\ DW)}$$

2.5. Soil DNA extraction and microbial community analysis (EMCA)

Soil DNA in 0.5 g of deeply frozen soil sample was extracted by the MoBioDNeasy Power Soil DNA isolation Kit (QIAGEN Inc., USA) according to the manufacturer's protocol. A Nanodrop-2000c spectrophotometer (Thermo Scientific, Wilmington, USA) was used to determine the quality and concentration of DNA. The target DNA fragment was obtained by PCR with 16S universal primers, and the sequence of 16S rDNA was about 1400 bp. The pooled DNA products were submitted to an Illumina MiSeq platform (Shanghai Biozeron). QIIME software (version 1.17) was used to test the original data and then to coordinate the effective sequence for subsequent analysis. UPARSE (version 7.1 http:// drive5. Com/uparse/) was used for OTU (operational taxonomic unit) classification and 97% sequence similarity was used for clustering. RDP classifier (http://rdp.cme.msu.edu/) and Silva (SSU123) 16S rDNA were used to summarize the abundance of taxa at different taxonomic levels (e.g., phylum, class, order, family, genus, and species).

2.6. Data quality control and assurance

All materials were cleaned with water and 98% alcohol after sample processing to be free of cross contamination. To assure the quality of THg and MeHg analysis, extraction and analyses of standard reference materials GSS-5, BCR-482, CC580 and TORT-3 were employed. The THg and MeHg recoveries for GSS-5, BCR-482, CC580 and TORT-3 were 95% to 102%, 97 to 103%, 94% to 101% and 95 to 102% (each standard has three replicates), respectively. The relative standard deviations for duplicate samples were within 6% and 8% for THg and MeHg, respectively. All data were performed using IBM SPSS (version 22.0) and plotted using Origin (version 9.0). One-way ANOVA and the LSD were

carried out to comparing the significance of different treatment groups at $P < 0.05$. Lowercase letters marked in the figures indicated that there was significant difference among different treatments ($P < 0.05$).

3. Results and discussion

3.1. Characterization of biochar and soil

The RWB and RHB are alkaline with pH value of 10.67 and 7.93, respectively (Table S2). The higher alkalinity of RWB than RHB could be attributed to the higher content of base cations of the former than the latter. The content of total carbon in the RHB (53%) was higher than the RWB (36%), indicating a high carbonization of RHB. It has been reported that the stability of carbon in biochar to resistant decomposition is closely related to the condensation degree of aromatic carbon, which depends on the types of feedstock and pyrolysis temperatures (Singh et al., 2012). The aromaticity of biochar is usually indicated by H/C ratio, and its lower value means a high aromaticity and thus great stability of carbon in biochar. Here, the H/C of RHB is two times lower than RWB (Table S2), suggesting that carbon of RHB is more stable than RWB. This result further supports that RHB contained more stable carbon than RWB. The polarity and hydrophilicity of biochar are indicated by O/C and (O + N/C) ratio (Wang et al., 2007). The values of O/C and (O + N/C) of RWB were higher than that of RHB, suggesting that the former biochar was more favorable for reactions with polar compounds than the latter. The content of silicon in RWB is higher than RHB, as straw is enriched with more Si than hull. The contents of organic matter, nitrogen and sulfur of the two biochars were similar.

The morphologies of RWB and RHB, determined by SEM, reveal regular and porous structures in unordered alignment (Fig. S1). The surface of RWB is rougher than RHB, as shown by the smaller pore diameter of RWB than RHB. Thus, the specific surface area of RWB should be larger than RHB. The presence of porous and rough structures of biochar should be favorable for Hg adsorption.

The FTIR spectra of RWB and RHB shows the absorption bands assigned to the characteristic groups OH stretching of phenolic hydroxyl groups and chemisorbed water in RWB and RHB at 3437 and 3402 cm^{-1}, respectively (Fig. 1). The organic C-H stretching regions are present in the 2950–2850 cm^{-1} (Madejová et al., 2020; Slaný et al., 2019). The absorption band at 1647 cm^{-1} was resulted from the aromatic C═C and C═O bonds vibrations of carboxyl groups in RWB. A strong complex band at 1087 and 1072 cm^{-1} is attributed to the C—O stretching vibration (Parshetti et al., 2013; Sevilla and Fuertes 2009). Absorption band at 870 cm^{-1} belongs to polycyclic aromatic structures C═C and aromatic C-H vibration occurs at 790 cm^{-1} (Biniak et al., 1997; Zhao and Xia 2018). The presence of polycyclic aromatic structures C═C and aromatic C—H vibration further demonstrate the presence of aromatic compounds in biochar. The enrichment of hydroxyl groups in the two biochars might play important roles in Hg adsorption.

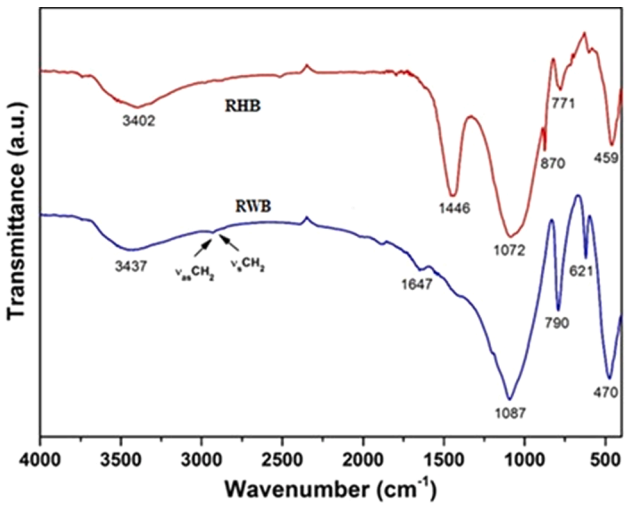

Fig. 1. FTIR spectra of rice–wheat straw biochar (RWB) and rice hull biochar (RHB).

The studied soil is weakly acidic with a pH value of 6.6 and contains low organic matter (2.9%) (Table S2). The contents of total carbon, nitrogen, and sulfur were 2.68%, 0.26%, and 0.05%, respectively. The total Hg concentration in the soil was 78.3 mg kg^{-1}, which exceeds the maximum allowable Hg contents in agricultural soil defined by Chinese government. It has been reported that inhabitant who live in Wanshan Hg mining area had been suffered from Hg exposure via rice consumption (Meng et al., 2014; Xia et al., 2020). Therefore, mitigation of Hg accumulation in rice is essential for minimizing human exposure to Hg.

3.2. Plant growth

The biomass of root and aboveground tissues increased by 18%-65% and 21%-119% in both biochar treatments as relative to corresponding controls, and their increases are clearer in high biochar dosage treatments (Fig. 2). The biochar-induced increase of the plant growth may be due to the input of organic matter and nutrients (e.g., PO_4^{3-}, K) into soils via biochar (Table S2), which is in agreement with other studies (Shu et al., 2016; Wang et al., 2020a; Wang et al., 2020b; Xing et al., 2020)

3.3. Effect of biochars on the soil microbial abundance

The microbial community composition was analyzed using 16 s rDNA gene sequencing. The relative abundance of *Proteobacteria* was much higher than *Euryarchaeota* and *Firmicutes*. Many bacteria in δ-Proteobacteria are sulfate and Fe(III)-reducing bacteria, which are able to convert Hg to MeHg (Gilmour et al., 2013; Parks et al., 2013). Bacteria possessing hgcA sequence mainly occurred in the phylum *Proteobacteria* (31.2–50.3%), *Firmicutes* (1–3%), and *Euryarchaeota* (0.37–0.62%) (Fig. S2). Fig. 3 shows the relative abundance of bacteria in genus that possess hgcA sequence in the five treatments after rice harvest. *Geobacter* was the predominant genus among all bacteria containing hgcA sequence in all five treatments. Application of 3% RWB to soil significantly ($P < 0.05$) increased hgcA genes abundance and diversity ($P < 0.05$), as compared to control. The increase of relative abundance of hgcA-carrying bacteria should be related to the increasing of carbon source by biochar amendments (Lehmann et al., 2011). The C/N had been linked to Hg methylation, here no clear relation between C/N and relative abundance of hgcA-carrying bacteria in soils were observed (Fig. S3), suggesting that the complicated Hg methylation process in soils after biochar amendment (Liu et al., 2018). RHB amendments did not clearly change the relative abundance of all hgcA-carrying bacteria. The difference in the relative abundance of hgcA-carrying bacteria between RWB and RHB treatments might be due to their different physicochemical properties (e.g., carbon content, labile organic matter) (Bruun et al., 2012), as indicated in a previous study which reported variable effects of biochars on microbial community composition (Zhang et al., 2019). The change of the relative abundance of hgcA-carrying bacteria by RWB amendment should have affected the methylation of Hg in the soil.

All soils share 2185 operational taxonomic units (OTUs), accounting for 47.4% of the total (Fig. S4). The number of unique OTUs in control, 0.6% RWB, 0.6% RHB, 3% RWB and 3% RHB were 315, 330, 282, 418 and 333, respectively. The RWB treatments had more unique OTUs than RHB treatments and control, suggesting that RWB might be more noticeable in enhancing microorganism activities.

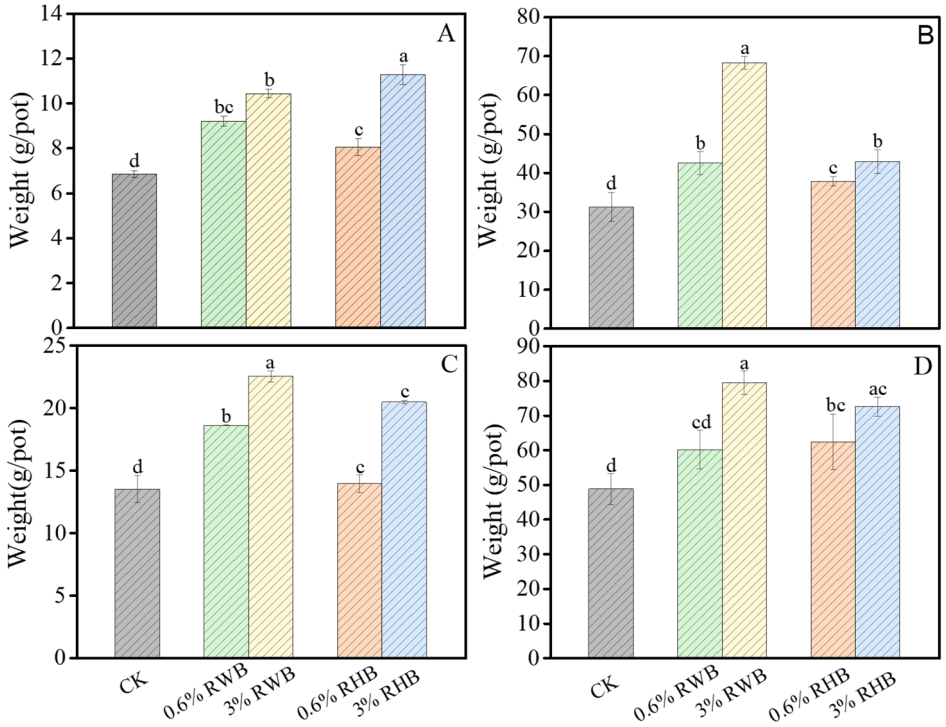

Fig. 2. The biomass of root (A), stalk (B), leaf (C) and grain (D) in control (CK), rice–wheat straw biochar (RWB) and rice hull biochar (RHB) treatments after rice harvest. The different lower-case letters on the bars indicate the difference between control and RWB/RWB treatment is significant at $P < 0.05$.

3.4. Biochars-induced change of THg, geochemical fractions of Hg, and MeHg in the soil

3.4.1. Total content and geochemical fractions of Hg

Addition of biochars caused a reduction in the concentrations of THg by 12% to 36% compared with control (Fig. 4-A), which should be attributed to dilution effect as a consequence of biochar amendment, and the heterogeneous conditions of soil.

The RWB and RHB affected the geochemical fractionation of Hg in the treated soil. The soluble and exchangeable and specifically-sorbed Hg fractions are potentially bioavailable for plants, and their reductions could inhibit plant uptake of Hg from soils. Biochar addition caused a significant decrease in the proportion of bioavailable Hg (soluble and exchangeable + specifically-sorbed Hg) by 62%-76% in the RHB treatment and by 69–79% in the RWB treatment as compared to the control (Fig. 5). The efficiency of biochar in reducing Hg bioavailability enhanced with increasing of the added dose (Fig. 5).

We assume two scenarios to underpin the mechanisms of Hg reduction by our biochars. Firstly, the large porosity of RWB and RHB (Fig. S1), and their enrichments in hydroxyl groups identified by FTIR (Fig. 1), might facilitate Hg adsorption. Secondly, the increase of pH in soil by biochar amendment may enhance Hg sorption and precipitation (Fellet et al., 2011; Gao et al., 2014).

The magnitude of reduction of soluble and exchangeable Hg in RWB treatments was greater than RHB treatments, which might relate to the different alkalinity of the two biochars (pH of RWB is 10.6, and RHB is 7.9), as the RWB-treated soil (7.3) had a higher pH than RHB (7.0). Mercury was prone to be immobilized under alkaline conditions. Biochars have strong cation exchange capacities (CECs) (Banik et al., 2018), and its amendment could enhance CEC (e.g., carboxylate and phenolate) of soil to adsorb Hg (Beckers et al., 2019; Cao et al., 2009; Gomez-Eyles et al., 2011).

There was no clear effect of RWB and RHB amendments on relative proportion of oxide-bound Hg. The relative proportions of organic-bound and residual Hg remained relatively unchanged in RHB and RWB treatments, as compared to control, which means that these Hg fractions were more resistant to pH and organic matter change caused by biochar amendment than soluble and exchangeable and specifically-sorbed Hg fractions.

The proportion of soluble and exchangeable and specifically-sorbed Hg fractions in control (CK) soil (after rice harvest) were ($P < 0.05$) higher than in bulk soil (before flooding), suggesting that both flooding and rice plant growth led to the mobilization of Hg in the soil, as reductive dissolution of Fe/Mn oxides could release the associated Hg, and plant root exuded organic compounds such as organic acids which reacted with soil minerals to liberate the associated metals (e.g., Hg) (Ko et al., 2008; Tao et al., 2004; Wang et al., 2011b). The mobilization of Hg in rhizosphere soil of *Chenopodium album* L after incubation for 60 days was reported (Wang et al., 2011a; Wang et al., 2011b). There was no significant difference in oxide-bound Hg, organic-bound Hg and residual Hg between control and bulk soil, suggesting that these fractions were poorly affected by rice plant growth.

3.4.2. Methylmercury

Amendment of RHB at two rates significantly ($P < 0.05$) decreased MeHg concentrations in the treated soil by 37.6–52.4% as compared to control, while of RWB at 3% noticeably increased MeHg concentrations in the soil (Fig. 4-B). Microbial-mediated reduction plays an important role in biogeochemical cycle of heavy metals in the environment (Chen et al., 2016). The production of MeHg is driven by microorganism (Xu et al., 2019). Available inorganic Hg substrate and active Hg-methylation bacteria determine MeHg production (Azaroff et al., 2020; Frohne et al., 2012; Schaefer et al., 2011). The change of MeHg concentration in a soil can be attributed to both of the alteration of Hg availability and/or activity of Hg-methylation bacteria. The RHB amendment did not significantly change the relative abundance of Hg-methylation bacteria, we therefore attributed MeHg decreasing to the reduced bioavailable Hg fractions (soluble and exchangeable + specifically-sorbed Hg), as the limited Hg was available for methylation (Liu et al., 2019d). Although bioavailable Hg fractions decreased in the RWB treatment, MeHg concentration even increased significantly in the soil (Fig. 4), which likely due to the increased relative abundance of Hg-

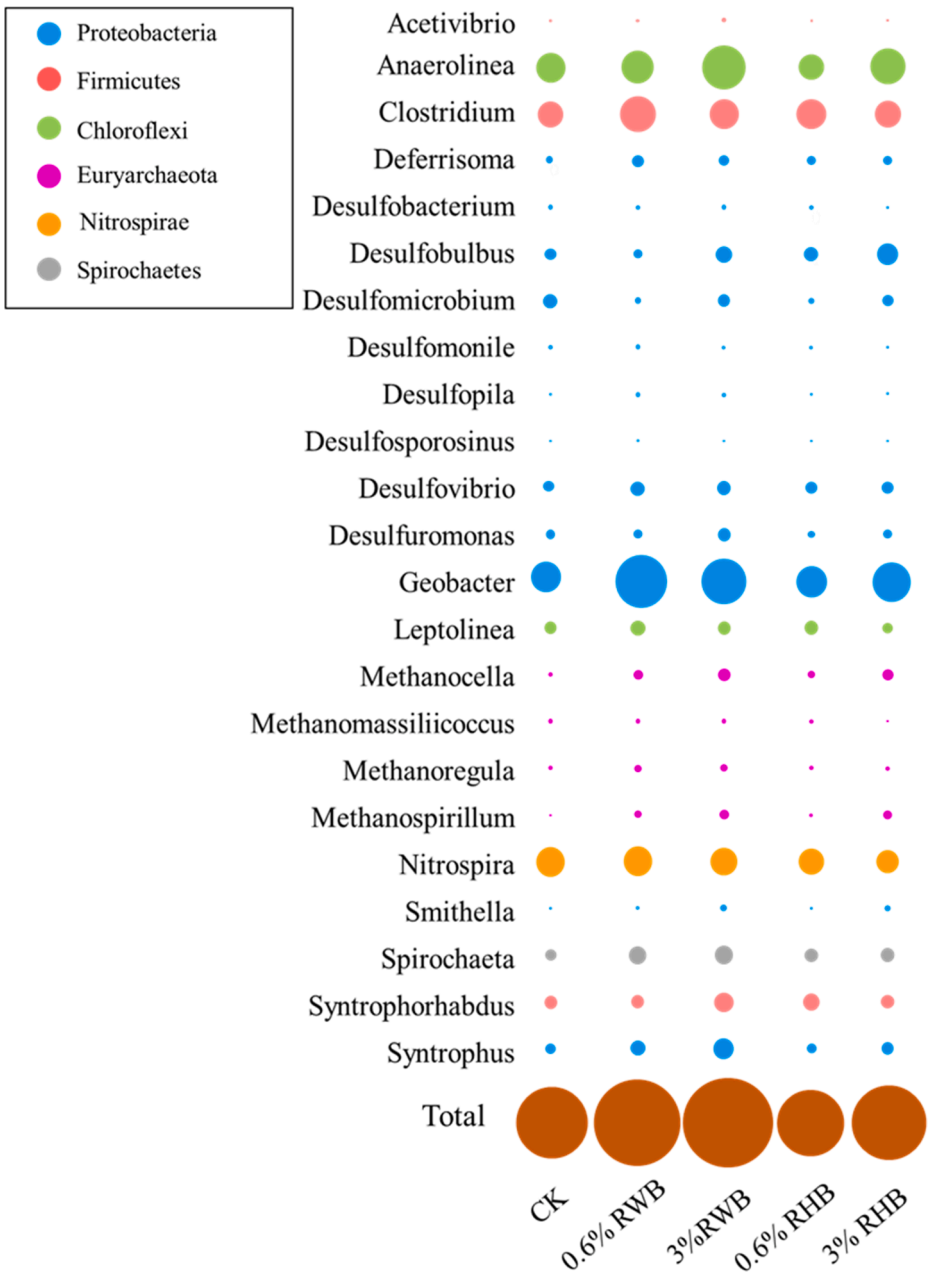

Fig. 3. Relative abundance of bacteria containing hgcA gene sequence at the genus level in control (CK), rice–wheat straw biochar (RWB) and rice hull biochar (RHB) treatments after rice harvest.

methylation microorganisms (e.g., *Geobacter* spp., *Nitrospira* spp.) as compared to the control and RHB treatments.

3.4.3. *Mercury in rice plants*

Application of both RWB and RHB at two rates significantly ($P < 0.05$) decreased THg concentrations in the roots compared to control (Fig. 6-A). However, the concentrations of THg in the stalk and leaf were poorly affected by the biochars amendment, except for 3% RWB treatment (Fig. 6-B and C). Our results were consistent with Xing et al. (2019) which reported that biochar amendment was more effective in reduction of Hg concentration in roots than leaves of rice. The concentration of THg in the polished rice in the control was 65 ng g^{-1} (Fig. 6-D), which was 3-fold higher than the maximum allowable Hg content in the grain (20 ng g^{-1}, GB2672-2017) defined by the State Food and Drug Administration of China. The concentrations of THg in the polished rice in the two biochar treatments decreased by 20–70% compared to control; in particular, 3% RWB-treated plant having THg concentration below 20 ng g^{-1}.

Although we observed a clear reduction of THg concentration in the roots, THg concentration in the aboveground tissues remained relatively stable. We calculated the absolute total Hg mass in the tissues of rice by multiplying Hg concentration by plant dry biomass. Mercury mass in the roots in all biochar treatments (except 3% RHB) was significantly ($0.05 > P$) lower than control (Fig S5, A). However, Hg masses in aboveground tissues were variable with biochar treatments. Mercury masses in the stalk, leaf and grain of RHB treatments were similar with corresponding controls (Fig S5, B-D), and that of RWB treatments depended on biochar application rate. The 0.6%RWB treatment had significantly higher Hg masses in the stalk and leaf than corresponding controls, while 3%RWB treatment showed an opposite phenomenon. Mercury mass in the grain in the two RWB treatments were significantly lower than control. These results demonstrated that 3%RWB reduced total Hg accumulation in the

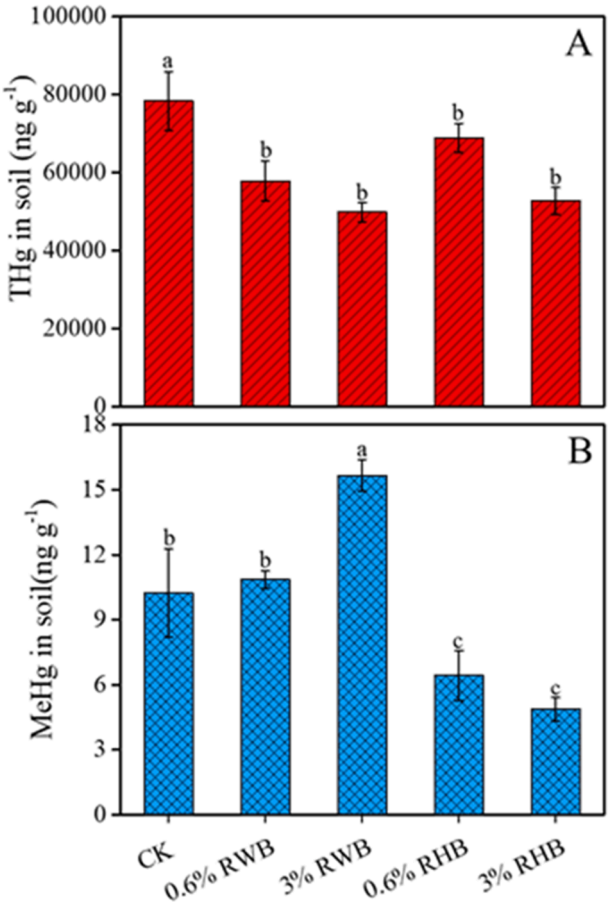

Fig. 4. The concentration of THg(A) and MeHg(B) in paddy soil in control (CK), rice–wheat straw (RWB) and rice hull biochar (RHB) treatments after rice harvest. The different lower-case letters on the bars indicate the difference between control and all biochar (RWB and RHB) treatments is significant at $P < 0.05$.

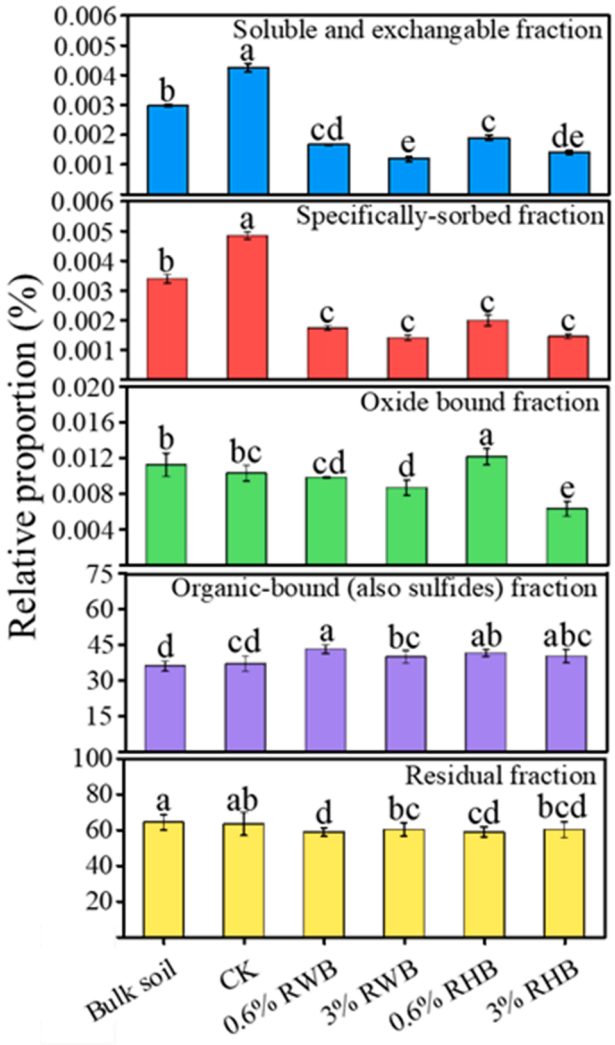

Fig. 5. The proportion of five fractions of Hg in control (CK), bulk soil, rice-straw (RWB) and rice hull biochar (RHB)-treated soils after rice harvest. The different lower-case letters on the bars indicate the difference in each Hg fraction between control and all biochar (RWB and RHB) treatments is significant at $P < 0.05$.

tissue of rice. However, RHB treatments poorly affected Hg in rice plants.

The effects of biochars amendment on MeHg reduction in rice tissues are more significant than THg (Fig. 6-E-H). The MeHg concentrations in the root, stalk, leaf and grain of rice plants decreased significantly up to 85%, 56%, 56% and 85%, respectively, in the biochar treatments compared with corresponding controls. Further, MeHg concentration in the roots decreased noticeably with the increasing applied dose of biochars ($P < 0.05$). Nevertheless, the concentration of MeHg in the stalk and leaf did not decrease as a function of biochar dose ($P > 0.05$). MeHg can be translocated from root to aboveground tissues of rice (Liu et al., 2019a). Herein, the decrease of MeHg concentration in the root may be responsible for the reduction of MeHg in the stalk and leaf. The lower MeHg concentration in the grain should be due to the decreased MeHg concentrations in the root, stalk, and leaf, as the translocation of MeHg from these tissues to grain was inhibited.

Fig S5 (E-H) showed the absolute MeHg mass in the tissues of rice plant. MeHg masses in the roots, stalks, leaves, and grains in all biochar treatments were significantly lower ($0.05 > P$) than corresponding controls, demonstrating that both RHB and RWB amendments were effective in reducing MeHg accumulation in rice plants. The underlying mechanisms for MeHg reduction in rice might be related to the decreased MeHg concentration in the soil, particularly for RHB treatments (Fig. 4). MeHg concentration in the soils increased with RWB amendment, but it decreased in the rice tissues. We attributed this phenomenon to the decreased phytoavailability of MeHg in soils due to binding of MeHg to organic sulfur groups in biochar and/or indirectly combined with organic sulfur species in soil (Shu et al., 2016; Wang et al., 2019; Wang et al., 2020c; Xing et al., 2020).

The bioaccumulation factor (BAF) and translocation factor (TF) of both THg and MeHg for rice are shown in Tables S3 and S4, respectively. Soil amendment with RWB decreased BAF_{MeHg} of the rice tissues compared with the control, showing that application of RWB reduced MeHg accumulation. Although RWB treatments increased MeHg concentration in the soil, the BAF_{MeHg} of rice plant decreased, as compared to control. The addition of RHB at two doses increased the BAF of MeHg in rice plants, especially at high treatment rate. The TF of MeHg for stalk to grain and leaf to grain decreased in both RWB and RHB amendments, suggesting a reduced translocation of MeHg within rice plant after biochars amendments. The addition of RWB reduced the TF of THg for root to grain, stalk to grain, and leaf to grain. Also, the BAF of THg for soil to root and soil to grain decreased after RWB amendment. These results suggested a limited translocation of MeHg in rice after biochar amendment.

We calculated the probable daily intake (PDI) of THg and MeHg via rice consumption for adult population (Table S5). The PDI of THg and MeHg was 0.349 and 0.256 μg kg^{-1}bw d^{-1}, respectively, for adult who might consume rice grown in un-treated soil (control). The PDI value for MeHg exceeds the reference dose of 0.1 μg kg^{-1}bw d^{-1} established by the

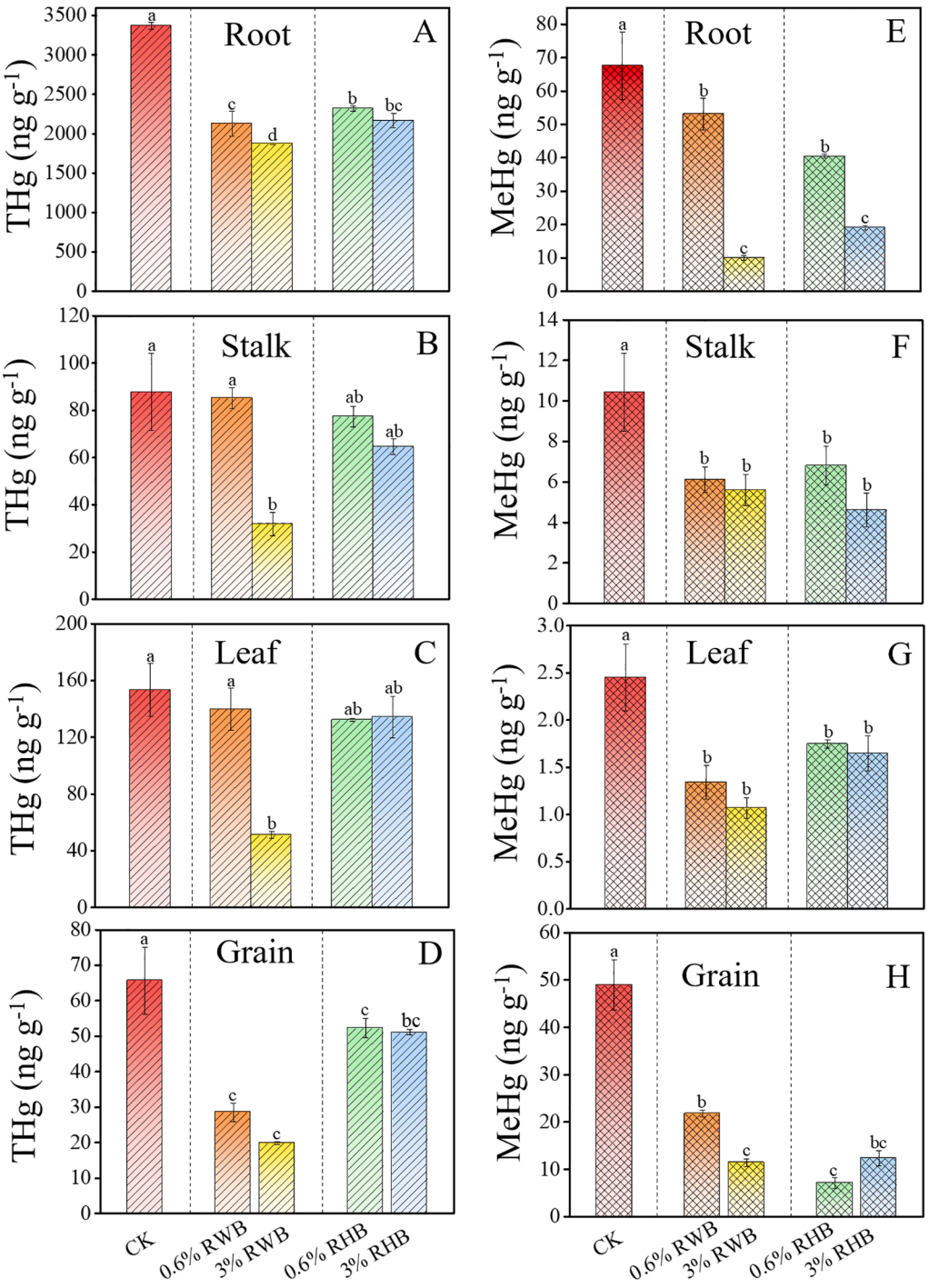

Fig. 6. The THg and MeHg concentration in different tissues of rice plants in control (CK), rice-straw biochar (RWB) and rice hull biochar (RHB) treatments after rice harvest. A, B, C, D represent THg concentration of root, stalk, leaf and grain, E, F, G, H represent MeHg concentration of root, stalk, leaf and grain. The different lower-case letters on the bars indicate the difference in root/stalk/leaf Hg concentration between control and all biochar (RWB and RHB) treatments is significant at $P < 0.05$.

USEPA (USEPA., 1997). while the PDI values of THg for adult population was below the provisional tolerable weekly intake (PTWI) of μg kg^{-1} bw $week^{-1}$ (equal to 0.57 μg kg^{-1}bw d^{-1}) (JECFA, 2010). The results demonstrated that rice consumption is one of routes of human exposure to MeHg at Wanshan Hg mining area. The RWB and RHB treatments significantly ($P < 0.05$) decreased PDI value of THg and MeHg by 20.2–69.7% and 55.5–85.4%, respectively, as compared with the corresponding controls. In particular, the PDI value of MeHg in most biochar treatments (except for 0.6% RWB treatment) was lower than the reference dose of 0.1 μg kg^{-1}bw d^{-1} defined by USEPA.

4. Conclusion

The application of biochar (i.e., RWB and RHB) significantly reduced the fraction of soluble and exchangeable and specifically-sorbed Hg (bioavailable Hg) in the soil as compared to control. The reduction of bioavailable Hg resulted in a limited bioavailable Hg for methylation. Consequently, we observed lower MeHg concentrations in the RHB-treated soil relative to the control. However, MeHg concentrations in the RWB-treated soil increased compared to the control, which should be attributed to the increased relative abundance of hgcA-carrying bacteria in the RWB treatments. The decreased total Hg concentration in the tissue of rice in both RWB and RHB treatments should be linked to the both the bio-dilution effects and Hg accumulation reduction by rice.

MeHg concentrations in the root, stalk, leaf, and grain of rice in both RWB and RHB treatments significantly decreased. We attributed these reductions to the decreased MeHg bioavailability in soils, and translocation within rice tissues.

Our results show a sustainable and economic way of recycling biowastes (e.g., rice hull, rice straw and wheat straw) by pyrolyzation to biochars, which is an important circular economy. Biochars can be used for remediation of Hg-polluted paddy soils. The studied biochars increased the biomass of rice plants, and this may encourage farmers to add biochar to soils to enhance rice plant yield. A large benefit accompanied with biochar application will be the reduction of Hg accumulation in rice grain. We found that the application of 3% RWB decreased the total Hg concentration in the grain to be lower than the recommended safe value of 20 ng g^{-1}, showing a very promising way of controlling Hg risks in paddy soils. Also, both RHB and RWB significantly decreased MeHg concentrations in the rice grain by 55–85%, which would mitigate the human health risk. The application of biochar to farmland at a rate of 3% is feasible, since such rate is often used to treat farmland with negligible negative effect on soil functions.

Our results demonstrate that RHB and RWB amendments may provide a novel and effective solution to remediate Hg-polluted farmlands in China and beyond. The production of biochar using feedstock that is in proximity with remedial regions may reduce the cost. Also, more studies are should be conducted under field conditions, aiming to explore biochars produced from different feedstock for an appropriate Hg remediation. Also, in future, the impact of redox fluctuations on the behavior of Hg in soils should be studied.

CRediT authorship contribution statement

Yi Man: Investigation, Data curation, Methodology, Validation, Writing - original draft, Writing - review & editing. **Bo Wang:** Investigation, Data curation, Visualization. **Jianxu Wang:** Investigation, Data curation, Conceptualization, Supervision, Funding acquisition, Writing - review & editing. **Michal Slaný:** Investigation, Validation. **Haiyu Yan:** Resources, Supervision, Funding acquisition. **Ping Li:** Resources, Funding acquisition, **Ali El-Naggar:** Writing - original draft. **Sabry M. Shaheen:** Visualization, Writing - review & editing. **Jörg Rinklebe:** Conceptualization, Writing - review & editing. **Xinbin Feng:** Funding acquisition, Conceptualization, Resources.

Declaration of Competing Interest

The authors declare that they have no known competing financial interests or personal relationships that could have appeared to influence the work reported in this paper.

Acknowledgment

This work was supported by the Strategic Priority Research Program of Chinese Academy of Sciences (XDB40020400), the Natural Science Foundation of China (42073081), Pioneer Hundred-Talent Program of Chinese Academy of Sciences and Nature Science Foundation of China [grant no 41703116], the Science and technology foundation of Guizhou Province [grant no ZK[2021]-key-045], the Social Development Project of Guizhou Province [Project No. [2012]3044]. Many thanks go to the Prof. Fangjie Zhao and Dr. Chuan Chen from Nanjing agricultural university for supporting by soil DNA extraction and sequencing.

Appendix A. Supplementary material

More details on the design of biochar production; pot experiment; the sequential extraction procedure; the calculated method of PDI; tables for properties of two biochars and soils; the bioaccumulation factor (BAF) and translocation factor (TF) of THg and MeHg in different tissues of control and biochar treatments(RWB and RHB); Figures showing the scanning electron microscopy of the biochar; the relative abundances of dominant Bacterial phyla; venn diagram of microorganism in soils; the absolute THg and MeHg values in different tissues of rice plants.

Supplementary data to this article can be found online at https://doi.org/10.1016/j.envint.2021.106527.

References

Azaroff, A., Urriza, M.G., Gassie, C., Monperrus, M., Guyoneaud, R., 2020. Marine mercury-methylating microbial communities from coastal to capbreton Canyon sediments (North Atlantic Ocean). Environ. Pollut. 262, 114333.
Banik, C., Lawrinenko, M., Bakshi, S., Laird, D.A., 2018. Impact of pyrolysis temperature and feedstock on surface charge and functional group chemistry of biochars. J. Environ. Qual. 47, 452–461.
Bao, Z., Wang, J., Feng, X., Shang, L., 2011. Distribution of mercury speciation in polluted soils of Wanshan mercury mining area in Guizhou. Chin. J. Ecol. 30, 907–913.
Beckers, F., Awad, Y.M., Beiyuan, J., Abrigata, J., Mothes, S., Tsang, D.C.W., Ok, Y.S., Rinklebe, J., 2019. Impact of biochar on mobilization, methylation, and ethylation of mercury under dynamic redox conditions in a contaminated floodplain soil. Environ. Int. 127, 276–290.
Beckers, F., Rinklebe, J., 2017. Cycling of mercury in the environment: sources, fate, and human health implications: A review. Crit. Rev. Environ. Sci. Technol. 47, 693–794.
Beesley, L., Moreno, E., Fellet, G., Carrijo, L., Sizmur, T., 2015. Biochar and heavy metals. In: Lehmann J., Joseph S., eds. Biochar for Environmental Management"Science, Technology and Implementation: Earthscan, London.
Biniak, S., Szymanski, G., Siedlewski, J., Swiatkowski, A., 1997. The characterization of activated carbons with oxygen and nitrogen surface groups. Carbon 35, 1799–1810.
Bruun, E.W., Ambus, P., Egsgaard, H., Hauggaard-Nielsen, H., 2012. Effects of slow and fast pyrolysis biochar on soil C and N turnover dynamics. Soil Biol. Biochem. 46, 73–79.
Buscaroli, A., 2017. An overview of indexes to evaluate terrestrial plants for phytoremediation purposes (Review). Ecol. Ind. 82, 367–380.
Cao, X., Ma, L., Gao, B., Harris, W., 2009. Dairy-manure derived biochar effectively sorbs lead and atrazine. Environ. Sci. Technol. 43, 3285–3291.
Chen, Z., Wang, Y., Xia, D., Jiang, X., Fu, D., Shen, L., Wang, H., Li, Q.B., 2016. Enhanced bioreduction of iron and arsenic in sediment by biochar amendment influencing microbial community composition and dissolved organic matter content and composition. J. Hazard. Mater. 311, 20–29.
Dong, X., Ma, L.Q., Zhu, Y., Li, Y., Gu, B., 2013. Mechanistic investigation of mercury sorption by brazilian pepper biochars of different pyrolytic temperatures based on X-ray photoelectron spectroscopy and flow calorimetry. Environ. Sci. Technol. 47, 12156–12164.
Driscoll, C.T., Mason, R.P., Chan, H.M., Jacob, D.J., Pirrone, N., 2013. Mercury as a global pollutant: sources, pathways, and effects. Environ. Sci. Technol. 47, 4967–4983.
El-Naggar, Ali, Lee, Mi-Hee, Hur, Jin, Lee, Young Han, Igalavithana, Avanthi Deshani, Shaheen, Sabry M., Ryu, Changkook, Rinklebe, Jörg, Tsang, Daniel C.W., Ok, Yong Sik, 2020. Biochar-induced metal immobilization and soil biogeochemical process: an integrated mechanistic approach. Sci. Total Environ. 698.
Fellet, G., Marchiol, L., Delle Vedove, G., Peressotti, A., 2011. Application of biochar on mine tailings: effects and perspectives for land reclamation. Chemosphere 83, 1262–1267.
Feng, X., Li, P., Qiu, G., Wang, S., Li, G., Shang, L., Meng, B., Jiang, H., Bai, W., Li, Z., Fu, X., 2008. Human exposure to methylmercury through rice intake in mercury mining areas, Guizhou Province, China. Environ. Sci. Technol. 42, 326–332.
Frohne, T., Rinklebe, J., 2013. Biogeochemical fractions of mercury in soil profiles of two different floodplain ecosystems in Germany. Water Air Soil Pollut. 224, 1591.
Frohne, T., Rinklebe, J., Langer, U., Du Laing, G., Mothes, S., Wennrich, R., 2012. Biogeochemical factors affecting mercury methylation rate in two contaminated floodplain soils. Biogeosciences. 9, 493–507.
Gamboa-Herrera, J.A., Rios-Reyes, C.A., Vargas-Fiallo, L.Y., 2020. Mercury speciation in mine tailings amended with biochar: effects on mercury bioavailability, methylation potential and mobility. Sci. Total Environ. 760, 143959.
Gao, Y., Liang, C., Pei, Z., Li, M., Xie, F., 2014. Effect of biochar and lime on the fraction transform of cadmium in contaminated soil. J. Soil Water Conserv. 28, 258–261.
Gilmour, C.C., Podar, M., Bullock, A.L., Graham, A.M., Brown, S.D., Somenahally, A.C., Johs, A., Hurt Jr., R.A., Bailey, K.L., Elias, D.A., 2013. Mercury methylation by novel microorganisms from new environments. Environ. Sci. Technol. 47, 11810–11820.
Gomez-Eyles, J.L., Sizmur, T., Collins, C.D., Hodson, M.E., 2011. Effects of biochar and the earthworm Eisenia Fetida on the bioavailability of polycyclic aromatic hydrocarbons and potentially toxic elements. Environ. Pollut. 159, 616–622.
He, L., Zhong, H., Liu, G., Dai, Z., Brookes, P.C., Xu, J., 2019. Remediation of heavy metal contaminated soils by biochar: mechanisms, potential risks and applications in China. Environ. Pollut. 252, 846–855.
Horvat, M., Lupsina, V., Pihlar, B., 1991. Determination of total mercury in coal fly-ash by gold amalgamation cold vapor atomic-absorption spectrometry. Anal. Chim. Acta. 243, 71–79.
Huang, Y., Wang, M., Li, Z., Gong, Y., Zeng, E.Y., 2019. In situ remediation of mercury-contaminated soil using thiol-functionalized graphene oxide/Fe-Mn composite. J. Hazard. Mater. 373, 783–790.
JECFA, 2010. The Joint FAO/WHO Expert Committee on Food Additives SeventySecond Meeting: Summary and Conclusions.

Jiménez-Moreno, M., Ángel Lominchar, M., José Sierra, M., Millán, R., Rodríguez Martín-Doimeadios, R.C., 2018. Fast method for the simultaneous determination of monomethylmercury and inorganic mercury in rice and aquatic plants. Talanta 176, 102–107.
Ko, B.-G., Anderson, C.W.N., Bolan, N.S., Huh, K.-Y., Vogeler, I., 2008. Potential for the phytoremediation of arsenic-contaminated mine tailings in Fiji. Aust. J. Soil Res. 46, 493–501.
Kong, H., He, J., Gao, Y., Wu, H., Zhu, X., 2011. Cosorption of phenanthrene and mercury(Ii) from aqueous solution by soybean stalk-based biochar. J. Agric. Food Chem. 59, 12116–12123.
Lahori, A.H., Guo, Z., Zhang, Z., Li, R., Mahar, A., Awasthi, M.K., Shen, F., Sial, T.A., Kumbhar, F., Wang, P., Jiang, S., 2017. Use of biochar as an amendment for remediation of heavy metal-contaminated soils: prospects and challenges. Pedosphere. 27, 991–1014.
Lee, S.H., Rhim, Y.J., Cho, S.P., Baek, J.I., 2006. Carbon-based novel sorbent for removing gas-phase mercury. Fuel 85, 219–226.
Lehmann, J., Rillig, M.C., Thies, J., Masiello, C.A., Hockaday, W.C., Crowley, D., 2011. Biochar effects on soil biota–a review. Soil Biol. Biochem. 43, 1812–1836.
Li, H., Dong, X., da Silva, E.B., de Oliveira, L.M., Chen, Y., Ma, L.Q., 2017. Mechanisms of metal sorption by biochars: biochar characteristics and modifications. Chemosphere 178, 466–478.
Li, P., Feng, X.B., Qiu, G.L., Shang, L.H., Li, Z.G., 2009. Mercury pollution in Asia: a review of the contaminated sites. J. Hazard. Mater. 168, 591–601.
Liang, L., Horvat, M., Cernichiari, E., Gelein, B., Balogh, S., 1996. Simple solvent extraction technique for elimination of matrix interferences in the determination of methylmercury in environmental and biological samples by ethylation gas chromatography cold vapor atomic fluorescence spectrometry. Talanta 43, 1883–1888.
Liu, J., Wang, J., Ning, Y., Yang, S., Wang, P., Shaheen, S.M., Feng, X., Rinklebe, J., 2019a. Methylmercury production in a paddy soil and its uptake by rice plants as affected by different geochemical mercury pools. Environ. Int. 129, 461–469.
Liu, M., Zhang, Q., Cheng, M., He, Y., Chen, L., Zhang, H., Cao, H., Shen, H., Zhang, W., Tao, S., Wang, X., 2019b. Rice life cycle-based global mercury biotransport and human methylmercury exposure. Nat. Commun. 10, 5164.
Liu, T., Wang, J., Feng, X., Zhang, H., Zhu, Z., Cheng, S., 2019c. Spectral insight into thiosulfate-induced mercury speciation transformation in a historically polluted soil. Sci. Total Environ. 657, 938–944.
Liu, Y.-R., Johs, A., Bi, L., Lu, X., Hu, H.-W., Sun, D., He, J.-Z., Gu, B., 2018. Unraveling microbial communities associated with methylmercury production in paddy soils. Environ. Sci. Technol. 52, 13110–13118.
Liu, Y.R., Yang, Z., Zhou, X., Qu, X., Li, Z., Zhong, H., 2019d. Overlooked role of putative non-Hg methylators in predicting methylmercury production in paddy soils. Environ. Sci. Technol. 53, 12330–12338.
Liu, Z., Chen, B., Wang, L.-a., Urbanovich, O., Nagorskaya, L., Li, X., Tang, L., 2020. A review on phytoremediation of mercury contaminated soils. J. Hazard. Mater. 400.
Madejová, J., Jankovič, Ľ., Slaný, M., Hronský, V., 2020. Conformation heterogeneity of alkylammonium surfactants self-assembled on montmorillonite: effect of head-group structure and temperature. Appl. Surf. Sci. 503, 144125.
Meng, B., Feng, X., Qiu, G., Anderson, C.W., Wang, J., Zhao, L., 2014. Localization and speciation of mercury in brown rice with implications for Pan-Asian Public Health. Environ. Sci. Technol. 48, 7974–7981.
Millán, R., Esteban, E., Zornoza, P., Sierra, M.-J., 2013. Could an abandoned mercury mine area be cropped? Environ. Res. 125, 150–159.
Ministry of Environmental Protection and Ministry of Land and Resources, 2014. China's Soil Pollution Status Bulletin edˆeds.
Muthayya, S., Sugimoto, J.D., Montgomery, S., Maberly, G.F., 2014. An overview of global rice production, supply, trade, and consumption. In: DeRegil, L.M., Laillou, A., MoenchPfanner, R., PenaRosas, J.P., eds. Technical Considerations for Rice Fortification in Public Health.
Namgay, T., Singh, B., Singh, B.P., 2010. Influence of biochar application to soil on the availability of as, Cd, Cu, Pb, and Zn to Maize (Zea Mays L.). Aust. J. Soil Res. 48, 638–647.
NRC, 2000. Toxicology Effects of Methylmercury edˆeds. National Academy Press, Washington, DC.
Palansooriya, K.N., Wong, J.T.F., Hashimoto, Y., Huang, L., Rinklebe, J., Chang, S.X., Bolan, N., Wang, H., Ok, Y.S., 2019. Response of microbial communities to biochar-amended soils: a critical review. Biochar 1, 3–22.
Pandey, S.K., Bhattacharya, T., Chakraborty, S., 2016. Metal phytoremediation potential of naturally growing plants on fly ash dumpsite of Patratu thermal power station, Jharkhand, India. Int. J. Phytoremediat. 18, 87–93.
Park, J.H., Choppala, G.K., Bolan, N.S., Chung, J.W., Chuasavathi, T., 2011. Biochar reduces the bioavailability and phytotoxicity of heavy metals. Plant Soil 348, 439.
Parks, J.M., Johs, A., Podar, M., Bridou, R., Hurt Jr., R.A., Smith, S.D., Tomanicek, S.J., Qian, Y., Brown, S.D., Brandt, C.C., Palumbo, A.V., Smith, J.C., Wall, J.D., Elias, D. A., Liang, L., 2013. The genetic basis for bacterial mercury methylation. Science 339, 1332–1335.
Parshetti, G.K., Hoekman, S.K., Balasubramanian, R., 2013. Chemical, structural and combustion characteristics of carbonaceous products obtained by hydrothermal carbonization of palm empty fruit bunches. Bioresour. Technol. 135, 683–689.
Podar, M., Gilmour, C.C., Brandt, C.C., Soren, A., Brown, S.D., Crable, B.R., Palumbo, A. V., Somenahally, A.C., Elias, D.A., 2015. Global prevalence and distribution of genes and microorganisms involved in mercury methylation. Sci. Adv. 1, 1–13.
Qasim, B., Motelica-Heino, M., 2014. Potentially toxic element fractionation in technosoils using two sequential extraction schemes. Environ. Sci. Pollut. Res. 21, 5054–5065.
Rothenberg, S.E., Windham-Myers, L., Creswell, J.E., 2014. Rice methylmercury exposure and mitigation: a comprehensive review. Environ. Res. 133, 407–423.
Schaefer, J.K., Kronberg, R.M., Morel, F.M.M., Skyllberg, U., 2014. Detection of a key Hg methylation gene, Hgca, in wetland soils. Environ. Microbiol. Rep. 6, 441–447.
Schaefer, J.K., Rocks, S.S., Zheng, W., Liang, L., Gu, B., Morel, F.M., 2011. Active transport, substrate specificity, and methylation of Hg(Ii) in anaerobic bacteria. Proc. Natl. Acad. Sci. U. S. A. 108, 8714–8719.
Sevilla, M., Fuertes, A.B., 2009. Chemical and structural properties of carbonaceous products obtained by hydrothermal carbonization of saccharides. Chemistry. 15, 4195–4203.
Shaheen, Sabry M, El-Naggar, Ali, Wang, Jianxu, Hassan, Noha E.E., Niazi, Nabeel Khan, Wang, Hailong, Tsang, Daniel C.W., Ok, Yong Sik, Bolan, Nanthi, Rinklebe, Jörg, 2019. Biochar as an (Im)mobilizing Agent for the Potentially Toxic Elements in Contaminated Soils. Biochar from Biomass and Waste: Fundamentals and Applications. Elsevier, pp. 255–274.
Shu, R., Wang, Y., Zhong, H., 2016. Biochar amendment reduced methylmercury accumulation in rice plants. J. Hazard. Mater. 313, 1–8.
Singh, B.P., Cowie, A.L., Smernik, R.J., 2012. Biochar carbon stability in a clayey soil as a function of feedstock and pyrolysis temperature. Environ. Sci. Technol. 46, 11770–11778.
Slaný, M., Jankovič, Ľ., Madejová, J., 2019. Structural characterization of organo-montmorillonites prepared from a series of primary alkylamines salts: Mid-Ir and near-Ir Study. Appl. Clay Sci. 176, 11–20.
Smith, S.D., Bridou, R., Johs, A., Parks, J.M., Elias, D.A., Hurt Jr., R.A., Brown, S.D., Podar, M., Wall, J.D., 2015. Site-directed mutagenesis of Hgca and Hgcb reveals amino acid residues important for mercury methylation. Appl. Environ. Microbiol. 81, 3205–3217.
Sommer, Y.L., Ward, C.D., Pan, Y., Caldwell, K.L., Jones, R.L., 2016. Long-term stability of inorganic, methyl and ethyl mercury in whole blood: effects of storage temperature and time. J. Anal. Toxicol. 40, 222–228.
Sparks, D.L., Page, A.L., Helmke, P.A., Loppert, R.H., Soltanpour, P.N., Tabatabai, M.A., Johnston, C.T., Summner, M.E., 1996. Methods of Soil Analysis. Part 3-Chemical Methods, 3rd Ed. Soil Science Society of America, Madison, WI.
Tao, S., Liu, W.X., Chen, Y.J., Xu, F.L., Dawson, R.W., Li, B.G., Cao, J., Wang, X.J., Hu, J. Y., Fang, J.Y., 2004. Evaluation of factors influencing root-induced changes of copper fractionation in Rhizosphere of a calcareous soil. Environ. Pollut. 129, 5–12.
Tessier, A., Campbell, P.G.C., Bisson, M., 1979. Sequential extraction procedure for the speciation of particulate trace-metals. Anal. Chem. 51, 844–851.
USEPA, 1997. Mercury Study Report to the Congress, Volume V: Health Effects of Mercury and Mercury Compounds. USEPA, Washington, DC, United States.
USEPA, 2001. Method 1630: Methyl Mercury in Water by Distillation, Aqueous Ethylation, Purge and Trap, and Cvafs edˆeds. USEPA, Washington, D.C., United States.
USEPA, 2002. Method 1631, Revision E: Mercury in Water by Oxidation, Purge and Trap, and Cold Vapor Atomic Fluorescence Spectrometry edˆeds. USEPA, Washington, D. C., United States.
Vishnivetskaya, T.A., Hu, H., Van Nostrand, J.D., Wymore, A.M., Xu, X., Qiu, G., Feng, X., Zhou, J., Brown, S.D., Brandt, C.C., Podar, M., Gu, B., Elias, D.A., 2018. Microbial community structure with trends in methylation gene diversity and abundance in mercury-contaminated rice paddy soils in Guizhou, China. Environ. Sci. Processes Impacts. 20, 673–685.
Wang, J., Feng, X., Anderson, C.W., Qiu, G., Ping, L., Bao, Z., 2011a. Ammonium thiosulphate enhanced phytoextraction from mercury contaminated soil-results from a greenhouse study. J. Hazard. Mater. 186, 119–127.
Wang, J., Feng, X., Anderson, C.W., Zhu, W., Yin, R., Wang, H., 2011b. Mercury distribution in the soil–plant–air system at the Wanshan mercury mining district in Guizhou, Southwest China. Environ. Toxicol. Chem. 30, 2725–2731.
Wang, J., Feng, X., Anderson, C.W.N., Wang, H., Wang, L., 2014. Thiosulphate-induced mercury accumulation by plants: metal uptake and transformation of mercury fractionation in soil - results from a field study. Plant Soil 375, 21–33.
Wang, J., Feng, X., Anderson, C.W.N., Xing, Y., Shang, L., 2012. Remediation of mercury contaminated sites - a review. J. Hazard. Mater. 221, 1–18.
Wang, J., Shaheen, S.M., Anderson, C.W.N., Xing, Y., Liu, S., Xia, J., Feng, X., Rinklebe, J., 2020a. Nanoactivated carbon reduces mercury mobility and uptake by Oryza Sativa L: mechanistic investigation using spectroscopic and microscopic techniques. Environ. Sci. Technol. 54, 2698–2706.
Wang, L., Hou, D., Cao, Y., Ok, Y.S., Tack, F.M.G., Rinklebe, J., O'Connor, D., 2020b. Remediation of mercury contaminated soil, water, and air: a review of emerging materials and innovative technologies. Environ. Int. 134, 105281.
Wang, X.R., Cook, S., Tao, S., Xing, B., 2007. Sorption of organic contaminants by biopolymer: role of polarity, structure and domain spatial arrangement. Chemosphere 66, 1476–1484.
Wang, Y., Dang, F., Zheng, X., Zhong, H., 2019. Biochar amendment to further reduce methylmercury accumulation in rice grown in selenium-amended paddy soil. J. Hazard. Mater. 365, 590–596.
Wang, Y., Sun, Y., He, T., Deng, H., Wang, Z., Wang, J., Zheng, X., Zhou, L., Zhong, H., 2020c. Biochar amendment mitigates the health risks of dietary methylmercury exposure from rice consumption in mercury-contaminated areas. Environ. Pollut. 267, 115547.
Wu, Q., Wang, S., Li, G., Liang, S., Lin, C.J., Wang, Y., Cai, S., Liu, K., Hao, J., 2016. Temporal trend and spatial distribution of speciated atmospheric mercury emissions in China during 1978–2014. Environ. Sci. Technol. 50, 13428–13435.
Xia, J., Wang, J., Zhang, L., Anderson, C.W.N., Wang, X., Zhang, H., Dai, Z., Feng, X., 2020. Screening of native low mercury accumulation crops in a mercury-polluted mining region: agricultural planning to manage mercury risk in farming communities. J. Cleaner Prod. 262, 121324.

Xing, Y., Wang, J., Shaheen, S.M., Feng, X., Chen, Z., Zhang, H., Rinklebe, J., 2020. Mitigation of mercury accumulation in rice using rice hull-derived biochar as soil amendment: a field investigation. J. Hazard. Mater. 388, 121747–121747.
Xing, Y., Wang, J., Xia, J., Liu, Z., Zhang, Y., Du, Y., Wei, W., 2019. A pilot study on using biochars as sustainable amendments to inhibit rice uptake of hg from a historically polluted soil in a Karst Region of China. Ecotoxicol. Environ. Saf. 170, 18–24.
Xu, J., Buck, M., Eklof, K., Ahmed, O.O., Schaefer, J.K., Bishop, K., Skyllberg, U., Bjorn, E., Bertilsson, S., Bravo, A.G., 2019. Mercury methylating microbial communities of boreal forest soils. Sci. Rep. 9.
Zhang, H., Feng, X., Larssen, T., Qiu, G., Vogt, R.D., 2010. In inland China, rice, rather than fish, is the major pathway for methylmercury exposure. Environ. Health Perspect. 118, 1183–1188.
Zhang, H., Sun, H., Zhou, S., Bai, N., Zheng, X., Li, S., Zhang, J., Lv, W., 2019. Effect of straw and straw biochar on the community structure and diversity of ammonia-oxidizing bacteria and archaea in rice-wheat rotation ecosystems. Sci. Rep. 9, 9367.
Zhang, L., Wang, S., Wang, L., Wu, Y., Duan, L., Wu, Q., Wang, F., Yang, M., Yang, H., Hao, J., Liu, X., 2015. Updated emission inventories for speciated atmospheric mercury from anthropogenic sources in China. Environ. Sci. Technol. 49, 3185–3194.
Zhao, Y., Xia, W., 2018. Recent Advances in Radical-Based C-N Bond Formation Via Photo-/Electrochemistry. Chem. Soc. Rev. 47, 2591–2608.